MAG: The Fluxgate Magnetometer of Venus Express

T.L. Zhang[1], G. Berghofer[1], W. Magnes[1], M. Delva[1], W. Baumjohann[1], H. Biernat[1], H. Lichtenegger[1], R. Nakamura[1], K. Schwingenschuh[1], H.-U. Auster[2], K.-H. Fornacon[2], I. Richter[2], K.-H. Glassmeier[2], C. Carr[3], A. Balogh[3], S. Barabash[4], K. Kudela[5], M. Balikhin[6], C.T. Russell[7], U. Motschmann[8] & J.-P. Lebreton[9]

[1]*Institut für Weltraumforschung (IWF), Austrian Academy of Sciences, A-8042 Graz, Austria*
Email: tielong.zhang@oeaw.ac.at
[2]*Institut für Geophysik und extraterrestrische Physik (IGEP), TU Braunschweig, Mendelssohnstr. 3, D-38106 Braunschweig, Germany*
[3]*Imperial College, London, Prince Consort Road, London SW7 2BW, UK*
[4]*Swedish Institute of Space Physics (IRF), Box 812, SE-981 28 Kiruna, Sweden*
[5]*Institute of Experimental Physics, Watsonova 47, 04353 Kosice, Slovakia*
[6]*University of Sheffield, Western Bank, Sheffield S10 2TN, UK*
[7]*Institute of Geophysics & Planetary Physics (IGPP), University of California, Los Angeles, CA 90024-1567, USA*
[8]*Institut für Theoretische Physik, TU Braunschweig, Mendelssohnstr. 3, D-38106 Braunschweig, Germany*
[9]*Research & Scientific Support Dept., European Space Agency, ESTEC, PO Box 299, 2200 AG Noordwijk, The Netherlands*

The MAG (Magnetometer) instrument of Venus Express is investigating the plasma environment of Venus. Although Venus has no intrinsic magnetic moment, its magnetic field plays an important role in the interaction of the solar wind with the planet. The hardware, with heritage from the ROMAP Rosetta Lander magnetometer, consists of two sensors, an electronics box and a carbon fibre boom. One sensor is located on the tip of the boom, while the other is mounted on the spacecraft body; this configuration allows the magnetic effects of spacecraft origin to be separated from the ambient space magnetic field.

1. Introduction

Venus, like other planets of the Solar System, is under the influence of a continuous flow of charged particles from the Sun: the solar wind (Russell & Vaisberg, 1983; Luhmann, 1986; Phillips & McComas, 1991). However, the lack of an intrinsic magnetic field makes Venus a unique object for studying the interaction between the solar wind and a planetary body. Venus has a dense atmosphere but no magnetic field, so the solar wind interacts directly with the upper atmosphere. The highly electrically conducting ionosphere deflects the supersonic solar wind around the planet so that a bow shock is formed. The interaction of post-shock solar wind flow with the ionosphere results in a distinct boundary – the ionopause. This separates the thermal plasma of the ionosphere from the hot magnetised plasma of the magnetosheath, which is defined as the region between the ionopause and bow shock.

The absence of a planetary magnetic field leads to important differences with the atmospheric-escape and energy-deposition processes at Earth. The direct interaction with the solar wind at Venus means that a large portion of the exosphere resides in the shocked solar wind flow; photoionisation, charge

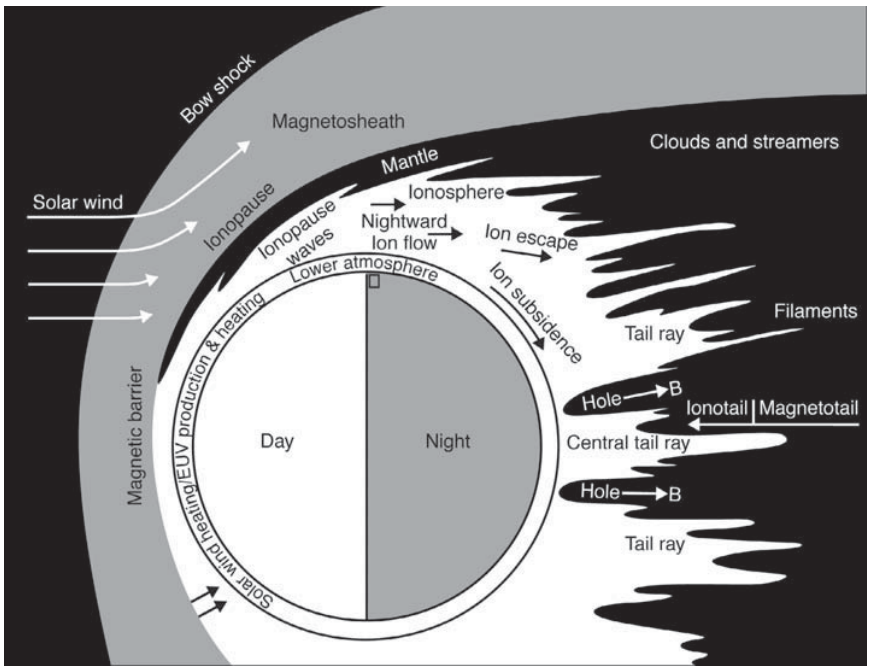

Fig. 1. Venus plasma environment during solar maximum as observed by Pioneer Venus Orbiter (after Brace et al., 1983). Since Venus Express arrived during solar minimum, it is seeing a different plasma environment.

exchange and electron impact ionisation remove ionised exospheric components via plasma flow. Another type of atmospheric loss arises from the tailward convection of the plasma mantle, situated between the shocked solar wind flow and the ionosphere. Ions gyrating around the magnetic field lines embedded in the plasma may reenter the atmosphere, causing extensive sputtering. Finally, erosion of the Venusian ionosphere under varying solar wind conditions provides an additional loss mechanism. The solar wind interacts with the top of the ionosphere to form a complex array of plasma clouds, tail rays, filaments and ionospheric holes on the nightside, through which a substantial amount of material leaves the planet. Fig. 1 illustrates the associated electrodynamics processes and plasma domains of the upper ionosphere, as derived from Pioneer Venus Orbiter (PVO) observations during solar maximum.

From the earlier Venera and PVO missions, it was found that the current induced by the solar wind electric field forms a magnetic barrier, which deflects most of the solar wind flow around the planet and leads to the formation of a bow shock (Zhang et al., 1991). The ionosphere is terminated on the dayside, developing rapid anti-sunward convection and tail rays. However, the short lifetimes of the Venera-9 and -10 orbiters and the insufficient temporal resolution of the Pioneer plasma instrument did not allow a study of the mass exchange between the solar wind and the upper atmosphere, or energy deposition in the upper atmosphere, in sufficient detail.

The MAG instrument of Venus Express is enabling the following studies:

— determining how the solar wind interacts the Venus atmosphere at solar minimum;
— mapping with high time-resolution the magnetic properties in the magnetosheath, magnetic barrier, ionosphere and magnetotail;
— characterising the plasma boundaries between the various plasma regions;
— determining the strength and occurrence of electromagnetic waves associated with any atmospheric electrical discharge;

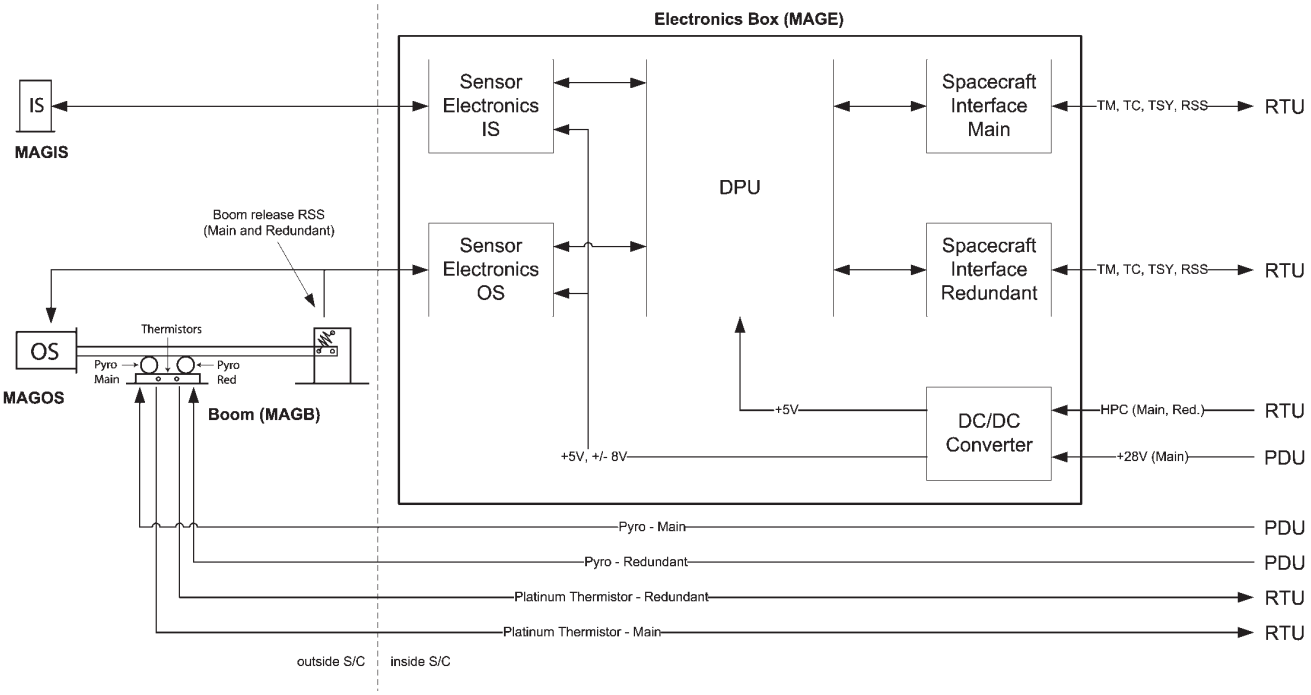

Fig. 2 (above). Block diagram of the Venus Express magnetometer. HPC: high power command, IS: inboard sensor, OS: outboard sensor, PDU: power distribution unit, RSS: relay status switch, RTU: remote terminal unit, TC: telecommand, TM: telemetry, TSYS: time synchronisation.

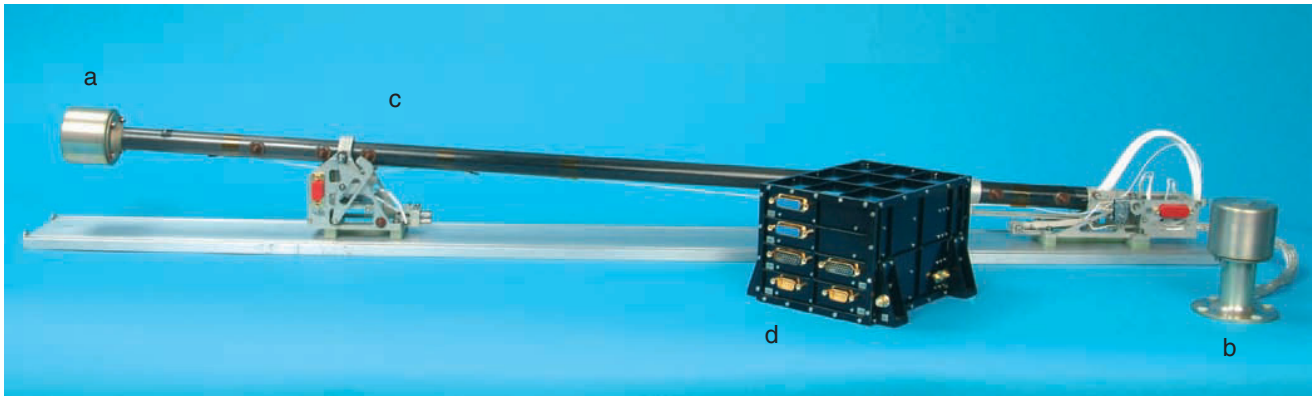

Fig. 3 (below). The Flight Model magnetometer. a: outboard sensor, b: inboard sensor, c: boom with launch lock and hinge, d: electronics box.

— providing supporting magnetic field data for particle observations of planetary ion pickup and similar processes.

2. The Instrument

2.1 Overview

MAG measures the magnetic field vector with a cadence of 128 Hz using two triaxial fluxgate sensors. The dual sensor configuration enables separation of stray field effects generated by the spacecraft from the ambient space magnetic field. The electronics box comprises two sensor electronics boards, the Data Processing Unit (DPU) board and the DC/DC power converter. The outboard sensor is mounted on the tip of a 900 mm-long carbon fibre deployed boom, while the inboard sensor is directly attached to the spacecraft with a separation of 10 cm from the +Z panel. The hardware benefits from the heritage of the

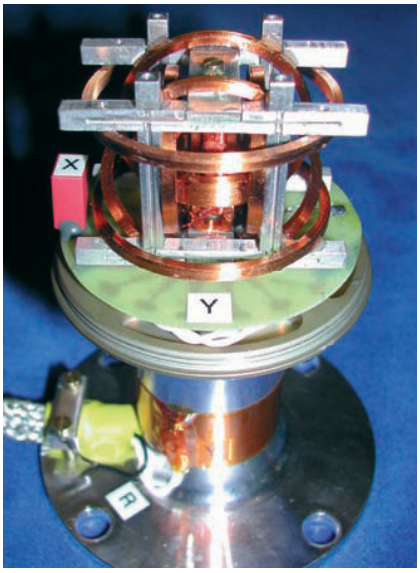

Fig. 4. The magnetometer sensor.

Table 1. The principal characteristics of MAG.

Range	±262 nT (default OS) ±524 nT (default IS)
Resolution	8 pT (default OS) 16 pT (default IS)
DC compensation	±10 000 nT
Data rate	2x128 Hz, 2x32 Hz, 2x1 Hz (OS and IS)
Telemetry	3328 bit/s or 104 bit/s
Power consumption	4.25 W max
Mass total: Electronics box Sensors Boom + hinge + launch lock MLI and harness	2308 g (incl. boom, harness and MLI) 992 g 75 g (OS) + 120 g (IS) 496 g 625 g
Size of electronics box	155 x 142 x 98.6 mm
Size of one sensor	~ 67 x 67 x 42 mm

IS: inboard sensor; OS: outboard sensor; MLI: multi-layer insulation

ROMAP Rosetta Lander magnetometer, which was commissioned in 2004. A block diagram of the instrument is shown in Fig. 2; the Flight Model (FM) is shown in Fig. 3. The instrument's key characteristics are given in Table 1.

2.2 Fluxgate sensors

Both fluxgate sensors (Fig. 4), featuring low mass and low power consumption, consist of two single ringcore sensors measuring the magnetic field in the X- and Y-axes. The magnetic field in the Z-axis is measured by a coil surrounding both single sensors. The sensor is identical to those of the Rosetta Lander and the Mir space station package, and similar to those flown on Equator-S (the same soft-magnetic ringcores made of an ultra-stable 6-81 Mo perm-alloy band, 2 x 20 mm). The ringcores have been tested under extreme environmental conditions on numerous space missions and in applied-geophysics situations. The excellent low-noise and stability behaviour of the sensor material was proved aboard Equator-S. The wide operating temperature range of the fluxgate sensor, from –160ºC to +120ºC, allows the sensor to be mounted on the outside of a temperature-controlled spacecraft, requiring only a passive multi-layer insulation blanket; no active heating or cooling is required.

2.3 Electronics

The sensor electronics (Fig. 5) generate an excitation AC current (fundamental frequency of ~9.6 kHz) to drive the soft magnetic core material deep into positive and negative saturation. According to the principle of fluxgate magnetometer operation, the external magnetic field distorts the symmetry of the magnetic flux and generates field-proportional even harmonics of the drive frequency in the sense coils.

The induced voltage in the sense coil is digitised immediately after the preamplifier at four times the excitation frequency. The 'front end' signal processing (synchronous detection and integration and calculation of the feedback signals) is performed by logic blocks within an Actel Field-Programmable Gate Array (FPGA; 54SX32). A feedback field increases the overall linearity and stability of the magnetometer. It is supplied to all sensor

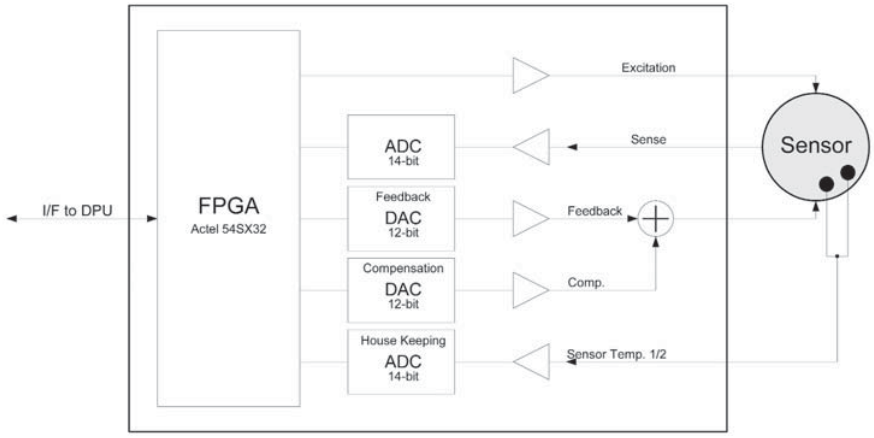

Fig. 5. Block diagram of the sensor electronics. ADC: analogue-to-digital converter, DAC: digital-to-analogue converter.

elements via 12-bit Digital-Analogue Converters (feedback DACs) and a separate pair of feedback coils (Helmholtz coils; Fig. 4) per sensor axis. Sense and feedback signals are continuously transmitted to the controller (128 Hz), which calculates the magnetic field values (24 bits) by scaling and adding the received data [(k1 x ADC) + (k2 x DAC)]. The appropriate dynamic range is defined by selecting and transmitting only bits of the calculated 24 bits (a kind of data compression). The range can thus be modified by telecommand between ±32.8 nT and ±8388.6 nT, with a corresponding digital resolution of between 1 pT and 128 pT. The default range for the outboard sensor is set to ±262 nT, with a resolution of 8 pT. The default range for the inboard sensor is ±524 nT. During operations, an artificial magnetic field of ±10 000 nT can be applied independently to each sensor via additional 12-bit DACs for compensation of any disturbing DC stray field.

The digital magnetometer concept of MAG requires analogue-to-digital conversion at a higher data rate but it provides a number of advantages over the more traditional analogue fluxgate magnetometer. Early digitisation makes the sensed signal robust against changes of the environmental temperature and the supply voltages, as well as insensitive to electromagnetic fields (Auster et al, 1995). Furthermore, no range switching is needed to achieve the full range at full resolution, which reduces design complexity and facilitates data analysis.

2.4 Data Processing Unit

The DPU controls the two sensors and the spacecraft interface and performs internal data-handling (sampling, data pre-processing, compression, data-frame generation). The DPU is based on an Intersil HS-RTX2010RH rad-hard microcontroller, which was specifically developed for embedded control in space systems. The controlling logic for the DPU, the sensor interfaces, the address decoder, the clock generator, the reset logic and the instrument spacecraft interface (standard ESA onboard data-handling interface) are implemented in an Actel 1020RH FPGA. A watchdog circuit, which is also implemented in the FPGA, continuously supervises the operation of the DPU and can release a cold start in case of a system crash. The DPU integrates 128 kbytes of static RAM, 64 kbytes of program memory (PROM) and 64 kbytes of electrically-erasable PROM (EEPROM). After power-on, the onboard software is copied to RAM. After this, the PROM is switched off and the instrument software is executed in RAM. This procedure reduces the DPU's power consumption. Software patches and various parameters can be uploaded to the instrument and stored in the EEPROM.

2.5 Power Supply Unit (DC/DC Converter)

The DC/DC Converter has design heritage from the units developed by Imperial College London (UK) for Cassini and Rosetta. For the Venus Express MAG instrument, a single (non-redundant) converter was provided. The +28 V main and redundant primary power inputs are therefore connected after the on/off relays. The converter provides four secondary supplies to MAG: +8 V and ±8 V to the analogue electronics, and a separate +5 V digital supply. Over-current protection is provided on the primary input side; the supply will automatically shut down in the event of an over-current. On the secondary side, the MAG electronics are protected by an over-voltage circuit, which will shut off the secondary side of the converter. The converter is stabilised with respect to changes in the load and changes in the input voltage, and is capable of maintaining the secondary voltages within the tight tolerances required by the electronics.

2.6 Deployable boom

The MAG boom has heritage from the Rosetta Lander magnetometer boom and was developed and fabricated by IGEP of TU Braunschweig (D). It consists of a 900 mm-long carbon fibre tube, a boom hinge and a launch lock. The MAG outboard sensor is mounted on the boom tip (Fig. 4). The boom release was initiated on 18 November 2005 by cable cutters (main and redundant), and the deployment was spring-driven. The launch lock was opened by a string cut by pyros. The boom is locked by a lever arm in the deployed position.

3. Measurements

3.1 Commands, modes and flight operation

MAG is based on the dual-magnetometer method to allow separation of the spacecraft stray field from the ambient space field (Ness et al., 1971). Both sensors take measurements simultaneously. MAG is operating continuously in

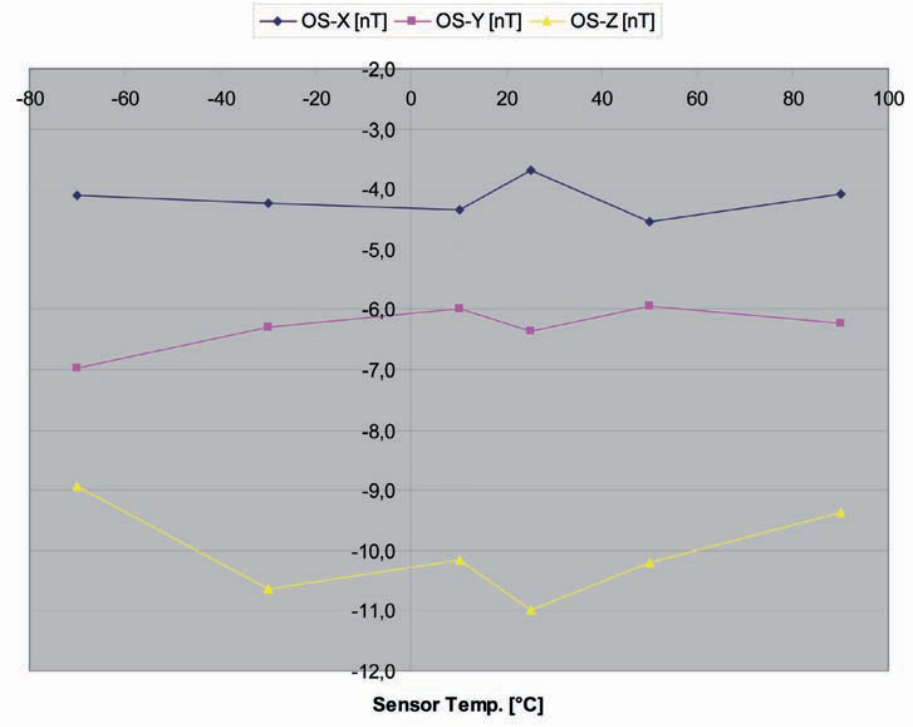

Fig. 6. Offset as a function of sensor temperature for the outboard sensor.

orbit around Venus and mostly in an autonomous mode, requiring little or no commanding. The nominal science modes are:

Instrument Mode	*Sensors*	*Data Rate*
Solar wind	OS and IS	1 Hz
Pericentre	OS and IS	32 Hz
Burst	OS and IS	128 Hz

After switching on, MAG automatically operates in a standard mode: solar wind mode with both sensors at 1 Hz data rate. During a typical science orbit, MAG is switched to pericentre mode an hour before pericentre, and then to solar wind mode an hour after pericentre. The instrument is commanded to the high-resolution burst mode a minute before pericentre for 2 min in order to detect lightning (Russell, 1991).

MAG was the first instrument to be commissioned on Venus Express, 10 days after launch, and its boom deployed. Afterwards, it remained ON during the commissioning of all the other instruments, to enable registration and characterisation of the magnetic disturbances generated during payload operation.

3.2 Instrument calibration and performance

Ground calibration of MAG was carried out at IWF Graz (A) and IGEP Braunschweig (D). The following calibration parameters of the Flight Model and Engineering Qualification Model were determined:

— scale factor, linearity and frequency response;
— noise of sensor and electronics;
— time stability of the sensor offset;
— temperature stability of sensor offset, instrument noise, linearity and scale factor;
— orthogonality of the triaxial sensor;
— crosstalk.

The instrument performed very well during ground calibration. At 1 Hz the noise density is less than 10 pT/√Hz for a sensor temperature range from 0ºC to +90ºC (the range in orbit around Venus) and the offset stability is better than 2 nT over the sensor temperature range from –75ºC to 90ºC (Fig. 6).

3.3 Magnetic survey of the spacecraft

It was not possible to investigate the magnetic cleanliness of the spacecraft and instruments to any great extent. Therefore, a problem to be solved for the magnetic field investigation is the determination of the magnetic stray fields (both DC and AC) from the spacecraft and payload. It is well known that these stray fields are generated primarily by a small number of potentially strong sources, such as thrusters, reaction wheels and solar panels. The magnetometer investigator team (mainly IWF Graz and IGEP Braunschweig), with long experience in magnetic cleanliness issues, undertook a magnetic examination programme to predict and determine the spacecraft stray fields at the sensors, using two different approaches.

At the spacecraft development level, a preliminary magnetic model of the spacecraft was constructed, based on the design and its payload accommodation, and by taking a representative set of known magnetic moments from equivalent subsystems and payload units on Rosetta and Mars Express. This model indicated a worst-case DC magnetic background of ~40 nT at the outboard sensor location and ~400 nT at the inboard sensor.

As a second step, magnetic measurements with a multiple gradiometer were performed during the different test phases of the assembled Mars Express and Venus Express spacecraft, with subsystems and elements of the payload in

operation. These measurements provided a description of the stray fields by means of model dipoles located on the spacecraft, indicating that the AC stray fields at the boom tip sensor are mainly in a range of 20–40 nT.

3.4 Data correction for spacecraft stray field effects

The measurements during flight are the sum of the ambient space field and stray fields from the spacecraft, with the space field the same at both sensors. When the magnetometers are well-calibrated, i.e. they perform identically, then any difference is attributable to the spacecraft.

If a single source is identified at a known position on the spacecraft, a model dipole field can be determined from the dual magnetometer measurement and subtracted to obtain the ambient space field. From this initial state, any change in the spacecraft effects is indicated by a change in the difference between the measurements at both sensors. In principle, identification of the disturbing source (and its temporal changes) from the in-flight telemetry enables a correction of the data for the stray field effects. Optimally, the corresponding model dipoles known from the ground survey can be used.

However, the Venus Express stray field effects are much more complicated and of a multi-dipole nature, so a combination of different methods is used. In the solar wind, well-known statistical methods, using time series of solar wind measurements, are used to determine an initial ambient space field level from the measurements at both sensors, with the data-difference only due to some initial state of the spacecraft effects. Temporal variations from this initial state are detected and, if possible, allotted to a single source on the spacecraft to allow correction.This method was successfully adopted for the Double Star project to remove routinely the solar panel disturbance in the magnetometer instrument data (Carr et al., 2005). In that case, the disturbances were clearly from the same source and had the same characteristics and pattern; they were visually identified and removed.

For Venus Express, routine manual identification of stray field patterns and their sources (known from the magnetic survey) and subsequent correction are beyond the resources of the MAG team. This raises the need for an automated correction procedure.

Since 2003, a new method of combining dual magnetometry and high-performance computation using neural networks has been under consideration. A neural network pattern-recognition algorithm was developed to identify stray field patterns in the differences of the magnetic field measurements at the sensors. A test algorithm was applied to simulated measurement data (ambient field and disturbance from up to seven simultaneous model dipoles), producing satisfactory results. The algorithm was successfully tested on real magnetic field measurements from Double Star. MAG data from the commissioning of the other instruments and the cruise data provided a ‘learning sequence” for the neural network algorithm. For the science data at Venus, a combination of the automated neural network algorithm and, in the worst case, correction by human resources is being applied.

4. The Team

The Venus Express magnetic field investigation involves an international team, led by the Institut für Weltraumforschung (IWF, Space Research Institute) of the Austrian Academy of Sciences in Graz. Other participants are the Technische Universität Braunschweig, Imperial College, London, the University of Sheffield, the Institute of Experimental Physics, Kosice, UCLA and IRF-Kiruna. Table 2 lists the investigator team and the responsibilities of the institutes.

Table 2. The Venus Express Magnetometer Team.

Investigators and team members	*Responsibilities*
Institut fur Weltraumforschung, Austrian Academy of Sciences, Graz	
T. Zhang (Principal Investigator) G. Berghofer (Experiment Manager) Co-Is: W. Baumjohann, H. Biernat, M. Delva, H. Lichtenegger, W. Magnes, R. Nakamura, K. Schwingenschuh Team members: E. Aydogar, H.U. Eichelberger, I. Jernej, K. Mocnik, W. Zambelli, Z. Voros	DPU, sensor electronics, onboard software, EGSE, integration, ground/in-flight calibration, boom qualification, environmental tests, magnetic examination programme, data processing/analysis
Institut fur Geophysik und extraterrestrische Physik, TU Braunschweig	
Co-Is: K.-H. Glalmeier, H.-U. Auster, K.-H. Fornacon, I. Richter Team members: K. Okrafka, B. Stoll	Sensor, sensor electronics, boom, boom qualification, ground/in-flight calibration, data processing/analysis, magnetic examination programme
Imperial College, London	
Co-Is: A. Balogh, C.M. Carr Team member: T. Beek	Power supply unit, electronics box enclosure, data processing/analysis
Institute of Experimental Physics, Kosice	
Co-I: K. Kudela Team members: G. Andrejkova, L. Hvizdos	Data processing/analysis
Institutet for Rymdfysik, Kiruna	
Co-I: S. Barabash	Data analysis
University of Sheffield	
Co-I: M. Balikhin	Data processing/analysis
University of California, Los Angeles	
Co-I: C.T. Russell	Data processing/analysis
Institut fur Theoretische Physik, TU Braunschweig	
Co-I: U. Motschmann	Theoretical modelling & data analysis
Research & Scientific Support Department, ESA/ESTEC, Noordwijk	
Co-I: J.-P. Lebreton	Data analysis

References

Auster, H.U., Lichopoj, A., Rustenbach, J., Bitterlich, H., Fornacon, K.-K., Hillenmaier, O., Krause, R., Schenk, H.J. & Auster, V. (1995). Concept and First Results of a Digital Fluxgate Magnetometer. *Meas. Sci. Technol.* **6**, 477–481.

Brace, L.H., Taylor Jr., H.A., Gombosi, T.I., Kliore, A.J., Knudsen, W.C. & Nagy, A. (1983). In *Venus* (Eds. D.M. Hunten, L. Colin, T.M. Donahue & V.I. Moroz), Univ. of Arizona Press, USA, pp779-840.

Carr, C., Brown, P., Zhang, T.L., Gloag, J., Horbury, T., Lucek, E., Magnes, W., O'Brien, H., Oddy, T., Auster, U., Austin, P., Aydogar, O., Balogh, A., Baumjohann, W., Beek, T., Eichelberger, H., Fornacon, K.-H., Georgescu, E., Glassmeier, K.-H., Ludlam, M., Nakamura, R. & Richter, I. (2005). The Double Star Magnetic Field Investigation: Instrument Design, Performance and Highlights of the First Year's Observation. *Ann. Geophys.* **23**, 2713–2732.

Luhmann, J. G. (1986). The Solar Wind Interaction with Venus. *Space Sci. Rev.* **44**, 241–306.

Ness, N.F., Behannon, K.W., Lepping, R.P. & Schatten, K.H. (1971). Use of Two Magnetometers for Magnetic Field Measurements on a Spacecraft. *J. Geophys. Res.* **76**, 3565–3573.

Phillips, J.L. & McComas, D.L. (1991). The Magnetosheath and Magnetotail of Venus. *Space Sci. Rev.* **55**, 1–80.

Russell, C.T. (1991). Venus Lightning. *Space Sci. Rev.* **55**, 317–356.

Russell, C.T. & Vaisberg, O. (1983). The Interaction of the Solar Wind with Venus. In *Venus* (Eds. D.M. Hunten, L. Colin, T.M. Donahue & V.I. Moroz), Univ. of Arizona Press, USA, pp873-940.

Zhang, T.L., Luhmann, J.G. & Russell, C.T. (1991). The Magnetic Barrier at Venus. *J. Geophys. Res.* **96**, 11145–11153.